

# Experimental Demonstration of Cognitive Spectrum Sensing & Notching for Radar

Jonathan W. Owen<sup>1</sup>, Brandon Ravenscroft<sup>1</sup>, Benjamin H. Kirk<sup>2</sup>, Shannon D. Blunt<sup>1</sup>, Christopher T. Allen<sup>1</sup>, Anthony F. Martone<sup>3</sup>, Kelly D. Sherbondy<sup>3</sup>, Ram M. Narayanan<sup>2</sup>

<sup>1</sup> Radar Systems Lab (RSL), University of Kansas, Lawrence, KS

<sup>2</sup> Electrical Engineering Dept., The Pennsylvania State University, University Park, PA

<sup>3</sup> Sensors and Electron Devices Division, Army Research Laboratory (ARL), Adelphi, MD

**Abstract**—A cognitive radar concept is demonstrated that incorporates spectrum sensing and subsequent waveform notching to avoid in-band interference. The interference is assumed to be caused by in-band orthogonal frequency division multiplexed (OFDM) communications in the vicinity of the radar while the notched radar waveform leverages a recently developed frequency modulated (FM) noise signal structure. To emulate real-time performance, the interference signal is measured as it hops in frequency and a fast spectrum sensing algorithm is applied to assess where notches are required. Knowledge of the determined notch location is then passed to the waveform optimization process. The interference and free-space radar measurements are synthetically combined to assess the impact of the interference with and without notching and to quantify the impact of latency.

**Keywords**—cognitive radar, spectrum sensing, FM noise, interference avoidance

## I. INTRODUCTION

With the expectation of continued growth in congestion in and around radar spectrum due to the proliferation of wireless devices [1,2] it is necessary for radar to explore ways in which interference can be avoided in a more proactive manner. As such, new policies and technologies are needed to allow radar to share spectrum with communication systems. Spectrum sharing technology offers the opportunity for radar to dynamically access the spectrum and mitigate mutual interference [3,4], one example of which is the cognitive radio paradigm [5]. This paradigm has likewise been extended to cognitive radar (e.g. [6-9]). Specifically, the perception-action cycle (PAC) depicted in Fig. 1 involves sensing the environment, deciding upon an appropriate action, and then adapting accordingly. We employ the PAC notion here to adapt the radar waveform to the interference environment.

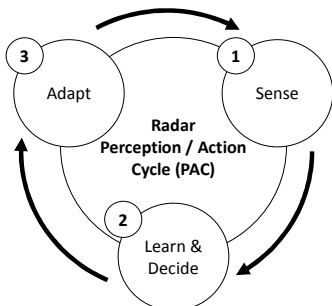


Figure 1: Perception-action cycle (PAC) concept for radar [5]

One such approach is through radio frequency interference (RFI) avoidance [10] via information gleaned from spectrum measurements of possible in-band interferers. Alternatively, we consider here how such information can realize wider bandwidths by spectral notching of radar waveforms (e.g. [11-22]). The learn/decide stage of this operation (per Fig. 1) is performed using the recently demonstrated fast spectral sensing (FSS) algorithm [23,24] that, in a manner mimicking the rapid data assimilation capability of the human thalamus [25], quickly determines the allowable spectrum bands. The FSS algorithm implements a threshold approach to first divide the spectrum into clusters of low and high power interference and then merges closely-spaced clusters into representative groups. This algorithm has been shown to significantly reduce the computational complexity of constrained optimization while maintaining solution accuracy [24].

Here FSS is used in conjunction with notched FM noise waveform design [20-22] with the ultimate goal of realizing real-time interference avoidance through spectrum notching. Using experimental loopback measurements of OFDM interference and separate free-space radar measurements obtained with the corresponding notched waveforms based on the FSS-estimated interference spectrum, the impact to the radar is evaluated by their synthetic combination. It is demonstrated that timely notching with these waveforms provides a significant signal to interference ratio (SIR) enhancement for moving target indication (MTI). This improvement is hindered, however, when there is latency in the update of notch spectral locations.

## II. SPECTRUM SENSING, SELECTION, & WAVEFORM DESIGN

In [23,24] a multi-objective optimization framework was proposed to determine the proper balance between contiguous radar bandwidth and the acceptable interference within that bandwidth. Decision latency is vitally important since the spectral landscape could change abruptly; thus the first stage of this optimization process involves a rapid band aggregation scheme that determines the contiguous spectral blocks that are available for use (individually).

The fast spectrum sensing (FSS) algorithm [23,24] was employed to identify the center frequencies and bandwidths of spectral regions that require notching. This approach first applies a threshold  $T_f$  to an observed discretized spectrum  $\Theta = \{\theta_1, \dots, \theta_N\}$  of sample size  $N$  to group the spectrum into meso-bands. A low power meso-band (LPM) is defined as a contiguous set of frequency samples below the threshold and a

high power meso-band (HPM) is a contiguous set of frequency samples above the threshold.

The  $q$ th meso-band is parameterized by start and end indices  $S(q)$  and  $E(q)$ , respectively. The number of frequency samples in each meso-band is  $L(q) = E(q) - S(q) + 1$ , which subsequently defines the associated bandwidth

$$B_q = L(q) \Delta f, \quad (1)$$

where  $\Delta f$  is the frequency resolution of  $\Theta$ . The FSS algorithm then enforces a minimum allowable bandwidth  $B_{\min}$  such that the radar spectrum is not too fragmented, as there is a need for a gradual transition into each notch to limit the attendant range sidelobes [26]. The minimum bandwidth is translated to the discrete frequency length

$$L_{\min} = \lceil B_{\min}/\Delta f \rceil, \quad (2)$$

for  $\lceil \cdot \rceil$  the ceiling operator. If an LPM has length  $L(q) \leq L_{\min}$ , then it is merged with adjacent HPMs to form the final set of low-power and high-power sub-bands. The radar may operate in the former and avoids the latter through the placement of spectral notches.

Given the available spectrum swaths within the radar bandwidth  $B$ , a sequence of FM noise waveform pulses is generated where each pulse *a*) is constant amplitude, *b*) adheres to a desired power spectrum  $|G(f)|^2$  that incorporates the required notches, and yet *c*) possesses a unique waveform. Here we use the pseudo-random optimized (PRO) FM framework that relies on alternating projection optimization [26,27], though very recently a gradient-based approach to FM noise radar spectrum notching has also been developed [28].

The generation of the  $m$ th FM noise waveform using PRO-FM involves the initialization of each pulse with a random instantiation of a polyphase-coded FM (PCFM) [29] waveform denoted as  $s_{0,m}(t)$ , followed by the alternating application of the projections

$$r_{k+1,m}(t) = \mathbb{F}^{-1} \left\{ |G(f)| \exp(j\angle \mathbb{F}\{s_{k,m}(t)\}) \right\} \quad (3)$$

$$s_{k+1,m}(t) = \exp(j\angle r_{k+1,m}(t)). \quad (4)$$

Here  $\mathbb{F}$  and  $\mathbb{F}^{-1}$  are the Fourier and inverse Fourier transforms, respectively, and  $\angle(\bullet)$  yields the phase of the argument. To realize low range sidelobes it is convenient to select a Gaussian shape for the power spectrum  $|G(f)|^2$ . The incorporation of spectral notches is then accomplished through the enforcement of the null constraints [20]

$$|G(f)| = 0 \text{ for } f \in \Omega, \quad (5)$$

where  $\Omega$  represents the frequency interval(s) of the notch(es).

To mitigate (partially) the  $\sin(x)/x$  roll-off in autocorrelation sidelobes that arises from the implicit rectangular notch definition in (5), it is also useful to employ a spectral taper in the regions surrounding each notch by also enforcing [21]

$$|G(f)| = \begin{cases} h_L(f) & \text{for } f \in \Omega_L \\ 0 & \text{for } f \in \Omega \\ h_U(f) & \text{for } f \in \Omega_U \end{cases}, \quad (6)$$

for  $\Omega_L$  and  $\Omega_U$  the frequency intervals of the lower and upper frequency taper  $h_L(f)$  and  $h_U(f)$ , respectively. These tapers are forced to be continuous with the surrounding power spectrum, thereby providing a gradual transition between the local spectrum and notch(es). Finally, because PRO-FM tends to achieve notch depths of only about 20 dB relative to the local values of  $|G(f)|^2$ , it has been shown [20,21] that the reiterative uniform weighted optimization (RUWO) method of [18] can be applied to the final version of the waveform to deepen the notches considerably.

### III. COGNITIVE RADAR DEMONSTRATION

We consider the situation in which the radio frequency interference (RFI) is an orthogonal frequency division multiplexed (OFDM) signal that is cohabitating the 3-dB bandwidth  $B$  occupied by the radar. This OFDM signal is modeled as consisting of eight adjacent subcarriers comprising a contiguous bandwidth of 10 MHz, with each subcarrier modulated by a random stream of quadrature amplitude modulated (QAM) symbols from a 4-QAM constellation.

To simplify the analysis, we consider a stationary radar performing moving target indication (MTI) such that platform motion effects such as angle-Doppler coupling of clutter and changing RFI direction need not be addressed. We wish to assess the performance of this radar mode experimentally when in the presence of the above communication RFI and with or without the use of cognitive spectral notching. Further, to isolate the impact of the spectral notch (which does incur a performance trade-off [22]) and the presence of the interference separately, the communication signal measurement and the free-space radar measurement are collected separately and then combined synthetically. Notch-free waveforms are likewise included to provide a performance baseline.

We consider three scenarios. In Case 1 the interference is stationary in frequency over the coherent processing interval (CPI). In Cases 2 and 3 the RFI changes, where the model in Fig. 1 is able to respond instantaneously in Case 2 but incurs a latency of one pulse repetition interval (PRI) for Case 3. The experimental timing diagram for Case 2 is illustrated in Fig. 2. Note that the full-band PRO-FM waveform and the notched PRO-FM waveform are interleaved such that both illuminate the same moving target scene for comparison. The RFI randomly hops to a new spectral location after every fourth PRI.

To facilitate the synthetic combination of communication and radar data, the OFDM signal is generated in Matlab and then captured in a loopback configuration using RF test equipment consisting of a Tektronix arbitrary waveform generator (AWG) and a Rohde & Schwarz real-time spectrum analyzer. The FSS algorithm is applied to this measured communication signal on a per-PRI basis to identify the occupied RFI band using a minimum continuous-band grouping requirement of 8 MHz. The results obtained from FSS are then used to adapt the notched PRO-FM waveforms according to the latency incurred (either none for Case 2 or one PRI for Case 3).

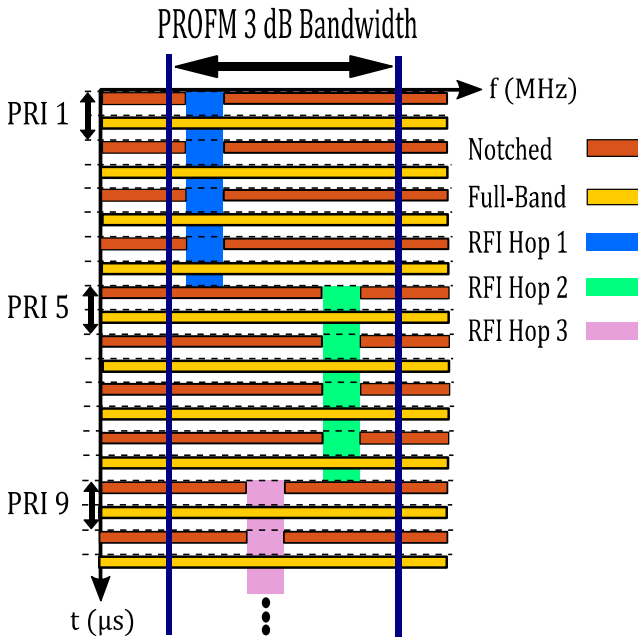


Fig. 2: Timing diagram for Case 2 (the radar adapts new notches instantly with changing interference location). The full-band and notched PRO-FM pulses are interleaved to provide the same MTI response.

The set of notched PRO-FM waveforms dictated by FSS were then transmitted (using the test setup in Fig. 3) from the roof of Nichols Hall on the KU campus to illuminate the intersection of 23<sup>rd</sup> St. and Iowa St. in Lawrence, KS. These open-air measurements were combined synthetically with the loopback-measured communications signals to assess overall performance.

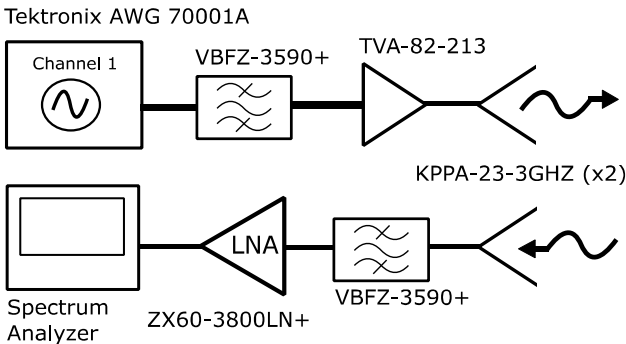


Fig. 3: Open-air hardware setup

For each case a total of 5000 interleaved pulses were transmitted, with 2500 each for full-band and notched PRO-FM. Accounting for the interleaving, the PRI is defined as the time period between each pair of pulses and is set to 40  $\mu$ s. Each pulse has a duration of 2  $\mu$ s and a 3-dB bandwidth of 100 MHz. Thus both sets of radar waveforms have time-bandwidth products of 200. The total CPI for each waveform set was 100 ms. The OFDM signals and radar emissions were each generated at a center frequency of 3.55 GHz and the resulting I/Q data were captured at a sample rate of 200 MHz for loopback and open-air measurements, respectively.

For radar receive processing, pulse compression matched filtering is performed using loopback captured versions of the emitted waveforms (also at 200 MHz sampling rate, or twice the 3-dB bandwidth) to account for hardware imperfections. Since there was no platform motion, clutter cancellation was performed by a simple projection of the zero-Doppler response and a Taylor taper was applied across Doppler.

To illustrate the measured spectra, Fig. 4 depicts the injected OFDM signal along with both the full-band and notched PRO-FM waveforms for a single pulse. The width of the observed notch arises from the fact that FSS identified some of the OFDM spectral roll-off as part of the region to avoid.

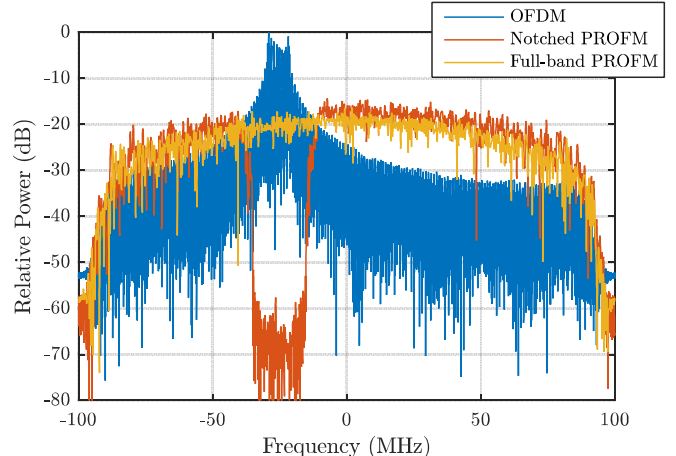


Fig. 4: The power-normalized measured spectra of the OFDM signal, notched PRO-FM (adapted using FSS), and full-band PROFM during 1 PRI

#### A. Case 1: Stationary Interference

As a baseline, Fig. 5 shows the measured range-Doppler response after clutter cancellation for the full-band PRO-FM waveform when no RFI is added. Multiple automobiles were traversing the intersection, which are clearly visible here as moving targets. It is useful to compare this result against the notched PRO-FM radar measurement without the inclusion of RFI as depicted in Fig. 6. A slight spreading in range is observed due to the presence of the notch, which agrees with the results obtained in [22]. Note that this effect is the result of higher near-in range sidelobes and not degraded resolution.

The OFDM RFI measured in loopback is power-scaled and then synthetically injected into the open-air test measurements. The “received” SIR is defined here as the root-mean-squared (RMS) power of the received radar backscatter signal (excluding direct path) divided by the RMS power of the OFDM interference within the time interval that the backscatter was received. A useful metric to assess the impact of interference as well as the hopping of spectral notches is

$$\Delta = \frac{I_{\text{meas}}}{I_{\text{baseline}}}, \quad (7)$$

where  $I_{\text{meas}}$  is the average power measured for each scenario in the range/Doppler regions separate from discernible targets and the clutter notch. The value  $I_{\text{baseline}}$  is then the value of  $I_{\text{meas}}$  for the full-band, no RFI scenario (e.g. Fig. 5).

Figures 7 and 8 show the range-Doppler plots for the full-band and notched PRO-FM when RFI is injected with a received SIR of  $-20$  dB. The full-band PRO-FM now experiences interference across all Doppler that realizes  $\Delta = 25$  dB. In contrast, the notched PRO-FM waveform only experiences about  $\Delta = 10$  dB of degradation, with many moving targets still evident. Note in Fig. 8 that background interference remains present due to RFI spectral leakage.

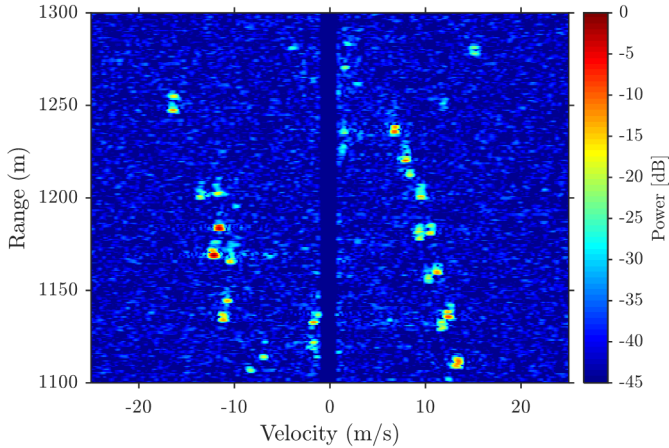


Fig. 5: Range-Doppler plot of full-band PROFM with no injected RFI (Case 1)

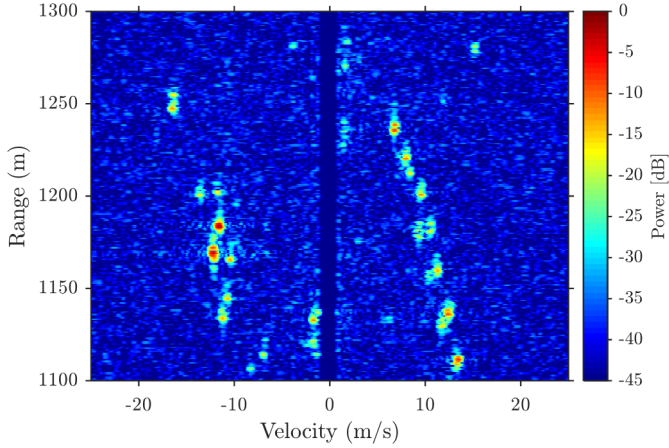


Fig. 6: Range-Doppler plot of notched PRO-FM with no injected RFI for Case 1 (obtained using stationary RFI)

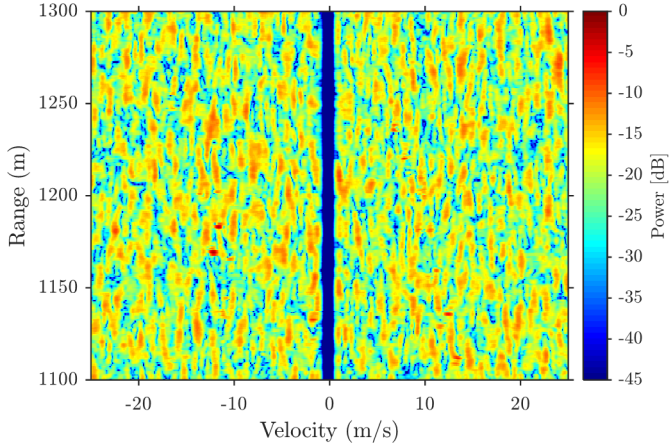


Fig. 7: Range-Doppler plot of full-band PRO-FM with injected stationary RFI of SIR =  $-20$  dB (Case 1)

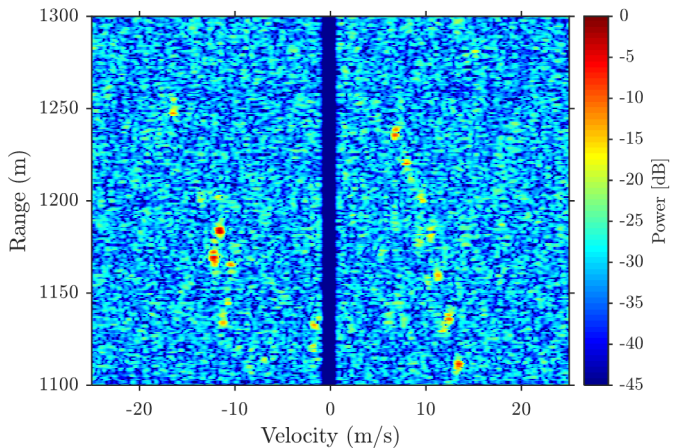


Fig. 8: Range-Doppler plot of notched PRO-FM with injected stationary RFI of SIR =  $-20$  dB (Case 1)

### B. Case 2: Hopped Interference, Instant Response

The hopped interference and notched waveforms in this case follow the timing arrangement depicted in Fig. 2, in which there is no latency between when the interference changes (every 4 PRIs) and when the notch location adjusts in response. Figures 9 and 10 show the full-band and notched PRO-FM responses when the RFI is not present, the former included to compare the same illuminated range-Doppler scene. The hopped frequency notches in Fig. 10 introduce a Doppler smearing effect that was noted in [21].

When the hopped RFI is present, again with a received SIR of  $-20$  dB, the full-band and notched PRO-FM responses in Figs. 11 and 12 are realized. The full-band response experiences the same  $\Delta = 25$  dB degradation as before. In contrast, the notched response now has about  $\Delta = 12$  dB of degradation, 2 dB more than the stationary interference scenario. While it is a bit difficult to see due to the different illuminated scenes and the Doppler smearing, it should be noted that Fig. 12 does not experience the higher near-in range sidelobes observed in Fig. 6 because the hopping of the notch destroys the coherency of those sidelobes.

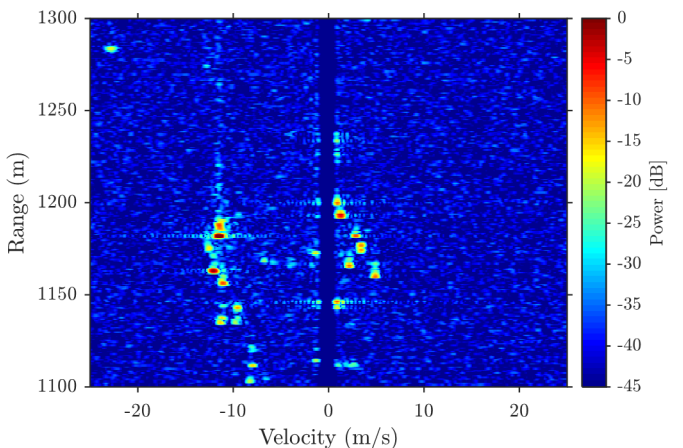


Fig. 9: Range-Doppler plot of full-band PROFM with no injected RFI (Case 2)

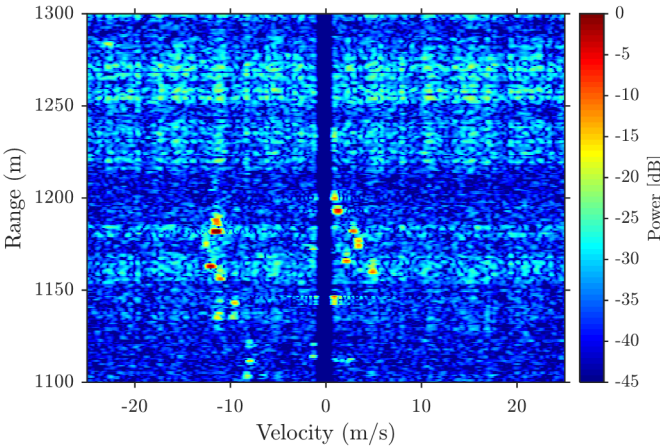


Fig. 10: Range-Doppler plot of notched PRO-FM with no injected RFI for Case 2 (frequency hopped RFI).

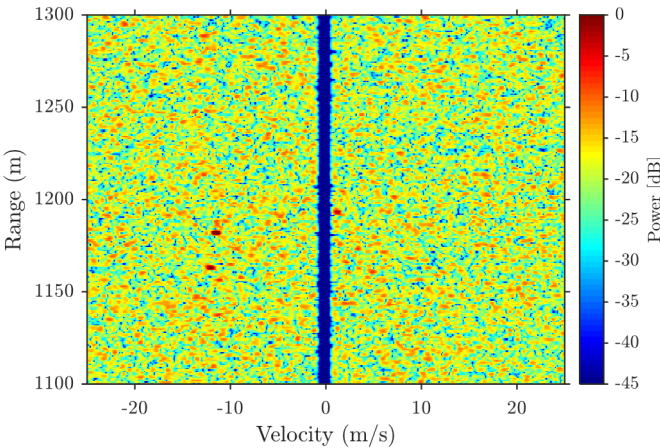


Fig. 11: Range-Doppler plot of full-band PRO-FM with injected frequency hopped RFI of SIR = -20 dB (Case 2)

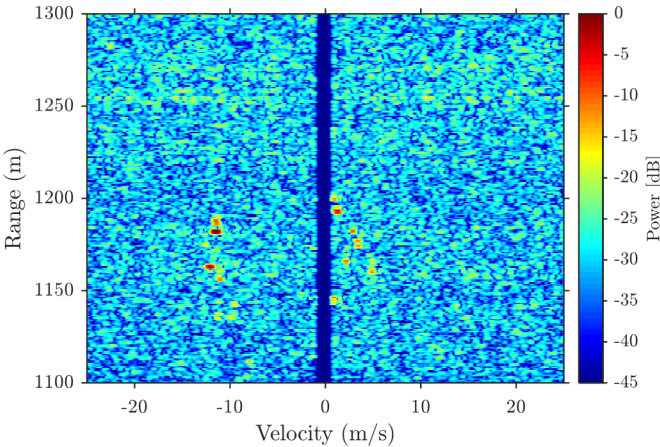


Fig. 12: Range-Doppler plot of notched PRO-FM with injected frequency hopped RFI of SIR = -20 dB (Case 2)

### C. Case 3: Hopped Interference, One PRI Response Latency

Finally, we examine the scenario in which there is a latency of one PRI before the location of the spectral notch can be determined (see Fig. 13). The RFI-free responses are omitted as they are qualitatively the same as observed in Figs. 9 and 10.

Figures 14 and 15 show the full-band and notched PRO-FM responses for this scenario. The full-band result is no different than before, with about  $\Delta = 25$  dB of degradation. Due to the perception-action cycle (PAC) latency, the notched case now experiences about  $\Delta = 17$  dB of degradation. This result emphasizes the importance of adapting the waveform to changing RFI as quickly as possible.

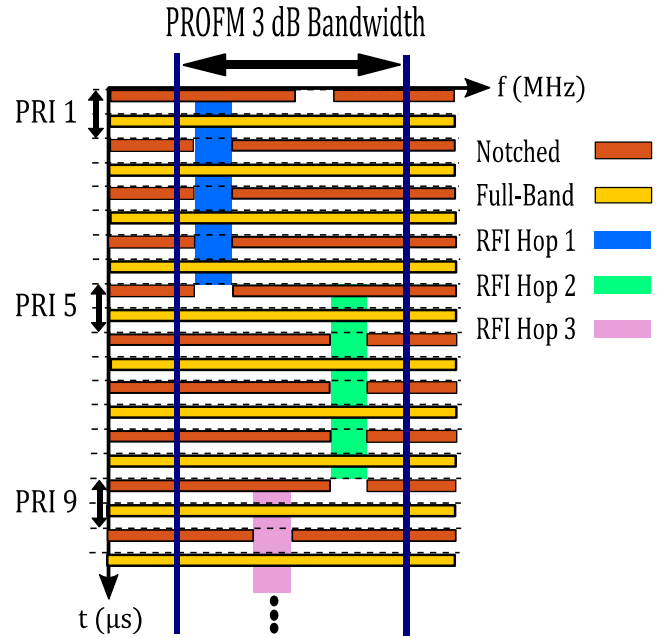


Fig. 13: Timing diagram for Case 3 (the PAC adapts new notches after a 1 PRI delay when the interference changes spectral location).

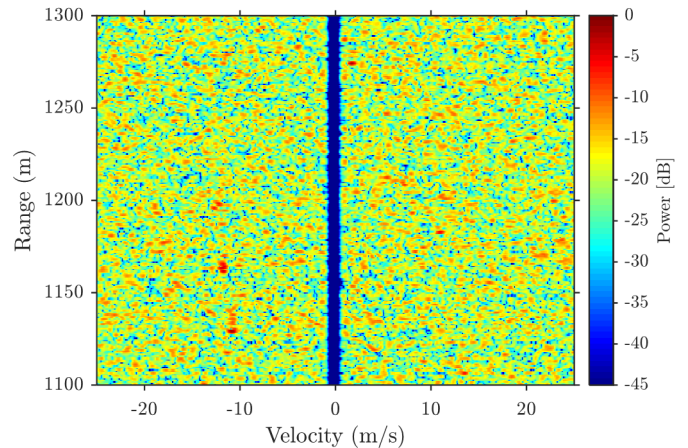


Fig. 14: Range-Doppler plot of full-band PRO-FM with injected frequency hopped RFI of SIR = -20 dB (Case 3)

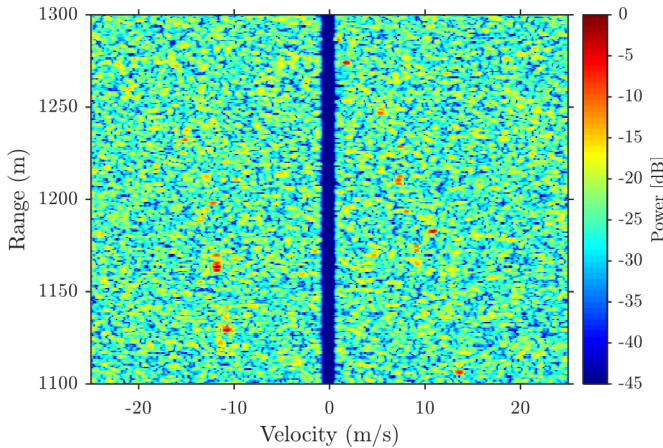


Fig. 15: Range-Doppler plot of notched PRO-FM with injected frequency hopped RFI of SIR = -20 dB and a one PRI latency (Case 3)

#### IV. CONCLUSIONS

It has been experimentally demonstrated using the synthetic combination of open-air radar measurements and loopback measurements of OFDM communication interference that cognitive spectrum sensing and notching can provide proactive interference avoidance. Compared to stationary interference, when frequency hopping of the interference occurs during the radar CPI a smearing of the Doppler response is observed. Further, latency to adjust the notch location(s) can degrade the output SIR.

#### REFERENCES

- [1] H. Griffiths, L. Cohen, S. Watts, E. Mokole, C. Baker, M. Wicks, S. Blunt, "Radar spectrum engineering and management: technical and regulatory issues," *Proc. IEEE*, vol. 103, no. 1, pp. 85-102, Jan. 2015.
- [2] M. Labib, V. Marojevic, A.F. Martone, J.H. Reed, A.I. Zaghloul, "Coexistence between communications and radar systems – a survey," to appear in *Radio Science Bulletin*.
- [3] J.M. Peha, "Sharing spectrum through spectrum policy reform and cognitive radio," *Proc. IEEE*, vol. 97, no. 4, pp. 708-719, Apr. 2009.
- [4] S.D. Blunt and E.S. Perrins, eds., *Radar & Communication Spectrum Sharing*, IET, 2018.
- [5] M. López-Benítez, "Sensing-based spectrum awareness in cognitive radio: challenges and open research problems," *Intl. Symp. Communication Systems, Networks & DSP*, Manchester, UK, July 2014.
- [6] S. Haykin, "Cognitive radar: a way of the future," *IEEE Signal Processing Mag.*, vol. 23, no. 1, pp. 30-40, Jan. 2006.
- [7] A.F. Martone, "Cognitive radar demystified," *URSI Bulletin*, no. 350, pp. 10-22, Sept. 2014.
- [8] K.L. Bell, C.J. Baker, G.E. Smith, J.T. Johnson, M. Rangaswamy, "Cognitive radar framework for target detection and tracking," *IEEE J. Selected Topics Signal Processing*, vol. 9, no. 8, pp. 1427-1439, Dec. 2015.
- [9] P. Stinco, M.S. Greco, F. Gini, "Spectrum sensing and sharing for cognitive radars," *IET Radar, Sonar & Navigation*, vol. 10, no. 3, pp. 595-602, Feb. 2016.
- [10] B.H. Kirk, K.A. Gallagher, J.W. Owen, R.M. Narayanan, A.F. Martone, K.D. Sherbony, "Cognitive software defined radar for time-varying RFI avoidance," submitted to *IEEE Radar Conf.*, Oklahoma City, OK, Apr. 2018.
- [11] M.J. Lindenfeld, "Sparse frequency transmit-and-receive waveform design," *IEEE Trans. Aerospace & Electronic Systems*, vol. 40, no. 3, pp. 851-861, July 2004.
- [12] M.R. Cook, T. Higgins, A.K. Shackelford, "Thinned spectrum radar waveforms," *Intl. Waveform Diversity & Design Conf.*, Niagara Falls, ON, Canada, Aug. 2010.
- [13] K. Gerlach, M.R. Frey, M.J. Steiner, A. Shackelford, "Spectral nulling on transmit via nonlinear FM radar waveforms," *IEEE Trans. Aerospace & Electronic Systems*, vol. 47, no. 2, pp. 1507-1515, Apr. 2011.
- [14] I.W. Selesnick and S.U. Pillai, "Chirp-like transmit waveforms with multiple frequency-notches," *IEEE Radar Conf.*, Kansas City, MO, May 2011.
- [15] C. Nunn, L.R. Moyer, "Spectrally-compliant waveforms for wideband radar," *Aerospace & Electronic Systems Mag.*, vol. 27, no. 8, pp. 11-15, August 2012.
- [16] L.K. Patton, B.D. Rigling, "Phase retrieval for radar waveform optimization," *IEEE Trans. Aerospace & Electronic Systems*, vol. 48, no. 4, pp. 3287-3302, October 2012.
- [17] L.K. Patton, C.A. Bryant, B. Himed, "Radar-centric design of waveforms with disjoint spectral support," *IEEE Radar Conf.*, Atlanta, GA, May 2012.
- [18] T. Higgins, T. Webster, A.K. Shackelford, "Mitigating interference via spatial and spectral nulling," *IET Radar, Sonar & Navigation*, vol. 8, no. 2, pp. 84-93, Feb. 2014.
- [19] A. Aubry, A. De Maio, Y. Huang, M. Piezzo, A. Farina, "A new radar waveform design algorithm with improved feasibility for spectral coexistence," *IEEE Trans. Aerospace & Electronic Systems*, vol. 51, no. 2, pp. 1029-1038, Apr. 2015.
- [20] J. Jakabosky, S.D. Blunt, A. Martone, "Incorporating hopped spectral gaps into nonrecurrent nonlinear FMCW radar emissions," *IEEE CAMSAP Workshop*, Cancun, Mexico, Dec. 2015.
- [21] J. Jakabosky, B. Ravenscroft, S.D. Blunt, A. Martone, "Gapped spectrum shaping for tandem-hopped radar/communications & cognitive sensing," *IEEE Radar Conf.*, Philadelphia, PA, May 2016.
- [22] B. Ravenscroft, S.D. Blunt, C. Allen, A. Martone, K. Sherbony, "Analysis of spectral notching in FM noise radar using measured interference," *IET Intl. Radar Conf.*, Belfast, UK, Oct. 2017.
- [23] A. Martone, K. Ranney, "Fast technique for wideband spectrum sensing," *IEEE Antennas & Propagation Int'l. Symp.*, Memphis, TN, July 2014.
- [24] A. Martone, K. Ranney, K. Sherbony, K. Gallagher, S. Blunt, "Spectrum allocation for non-cooperative radar coexistence," *IEEE Trans. Aerospace & Electronic Systems*, vol. 54, no. 1, pp. 90-105, Feb. 2018.
- [25] W.M. Connelly, M. Laing, A.C. Errington, V. Crunelli, "The thalamus as a low pass filter: filtering at the cellular level does not equate with filtering at the network level," *Frontiers in Neural Circuits*, vol. 9, no. 89, pp. 1-10, Jan. 2016.
- [26] J. Jakabosky, S.D. Blunt, B. Himed, "Spectral-shape optimized FM noise radar for pulse agility," *IEEE Radar Conf.*, Philadelphia, PA, May 2016.
- [27] J. Jakabosky, S.D. Blunt, B. Himed, "Waveform design and receive processing for nonrecurrent nonlinear FMCW radar," *IEEE Intl. Radar Conf.*, Arlington, VA, May 2015.
- [28] C.A. Mohr, P.M. McCormick, S.D. Blunt, C. Mott, "Spectrally-efficient FM noise radar waveforms optimized in the logarithmic domain," submitted to the *IEEE Radar Conf.*, Oklahoma City, OK, Apr. 2018.
- [29] S.D. Blunt, M. Cook, J. Jakabosky, J. de Graaf, E. Perrins, "Polyphase-coded FM (PCFM) radar waveforms, part I: implementation," *IEEE Trans. Aerospace & Electronic Systems*, vol. 50, no. 3, pp. 2218-2229, July 2014.